**Smart Structures and Systems**, *Vol. 15, No. 2 (2015) 283-297*
DOI: http://dx.doi.org/10.12989/sss.2015.15.2.283 

# Electromechanical impedance-based long-term SHM for jacket-type tidal current power plant structure

Jiyoung Min[1], Jin-Hak Yi[*2,3] and Chung-Bang Yun[4]

*[1]Structural Engineering Research Division, SOC Research Institute, Korea Institute of Civil Engineering and Building Technology, 283 Goyangdae-ro, Ilsanseo-gu, Goyang-si, Gyeonggi-do 411-712, Republic of Korea*
*[2]Coastal and Environmental Engineering Division, Korea Institute of Ocean Science and Technology, 787 Haean-ro, Sangnok-gu, Ansan, Gyeonggi-do 426-744, Republic of Korea*
*[3]Department of Convergence Study on the Ocean Science and Technology, Korea Maritime and Ocean University, Busan, Republic of Korea*
*[4]School of Urban and Environmental Engineering, Ulsan National Institute of Science and Technology, UNIST-gil 50, Ulsan 689-798, Republic of Korea*

*(Received May 1, 2014, Revised September 19, 2014, Accepted November 18, 2014)*

**Abstract.** Jacket-type offshore structures are always exposed to severe environmental conditions such as salt, high speed of current, wave, and wind compared with other onshore structures. In spite of the importance of maintaining the structural integrity for an offshore structure, there are few cases to apply a structural health monitoring (SHM) system in practice. The impedance-based SHM is a kind of local SHM techniques and to date, numerous techniques and algorithms have been proposed for local SHM of real-scale structures. However, it still requires a significant challenge for practical applications to compensate unknown environmental effects and to extract only damage features from impedance signals. In this study, the impedance-based SHM was carried out on a 1/20-scaled model of an Uldolmok current power plant structure in Korea under changes in temperature and transverse loadings. Principal component analysis (PCA)-based approach was applied with a conventional damage index to eliminate environmental changes by removing principal components sensitive to them. Experimental results showed that the proposed approach is an effective tool for long-term SHM under significant environmental changes.

**Keywords:** piezoelectric sensors; electromechanical impedance; temperature; load; structural health monitoring; principal component analysis

## 1. Introduction

Recently global warming is getting severe and natural disasters due to abnormal weather are successively threatening our lives and properties. It is a well-known that these problems are due to the excessive use of combustible fuel and excessive discharging of $CO_2$. Therefore most of countries are trying to develop the renewable energies such as biomass, wind, and solar to cope with the global warming and to replace the drained combustible energy. Even though the biomass, wind and solar energies are sharing most part of renewable energy market, the marine energy is

∗Corresponding author, Ph.D., Principal Research Scientist, E-mail: yijh@kiost.ac


http://www.techno-press.org/?journal=sss&subpage=8 ISSN: 1738-1584 (Print), 1738-1991 (Online)

certainly one of the most attractive and important energy sources in Korea because it is surrounded by the ocean on three sides. Korea especially has several potential sites where tidal current power plants can be constructed with the very high current speed of tides. Among them, Uldolmok strait is the most famous due to distinguish characteristics with high current speed and narrow and deep shape. Thus Korea Institute of Ocean Science and Technology (KIOST) constructed the Uldolmok Tidal Current Power Plant (TCPP) with funding of Ministry of Oceans and Fisheries since 2000, and the economic efficiency, construction, and maintenance of TCPP are going to be investigated after construction.

TCPP generally consists of a power generating system and its supporting system. The power generating system includes marine hydrokinetic turbines, generators, and power converters. The supporting system fixes the location of the power generating system for operation of TCPP. For Uldolmok TCPP, a jacket-type supporting system was selected among various types considering the efficiency, safety, economic feasibility, and workability. To minimize the size of main jacket legs, jacket legs were designed just to meet the minimum design criteria, and the manufacturing, assembling, and installation were precisely controlled with dimension control/measuring system and nondestructive testing. Unfortunately the TCPP is sometimes exposed to unexpected environments such as excessively high tidal current loads and salt in the ocean during operation and these reduce the structural safety inducing structural damages in critical members of the structure even though the construction was carefully carried out. Therefore the structural health monitoring (SHM)is required to monitor structural conditions and to alarm undesirable structural damages. However, because access to the TCPP is difficult and maintenance and repair works are limited, there are very few cases that the SHM system was applied to the TCPP. Most researches utilized strain data at joint connection, acceleration data with eigenvalue analysis, or slope data for structural damage evaluation. Several techniques were also proposed for compensating temperature effects with the ARX model and the cross-correlation coefficient. Actually deformations and damages can be occurred by environmental factors on seawater and atmosphere, boat collisions, current loads, corrosion, and fatigue so that it is critical to monitor and evaluate the structural condition with careful consideration for both temperature and external load variations for safe and efficient operation of whole TCPP system.

The SHM may be broadly categorized into two approaches by inspection domain: global SHM and local SHM. Global SHM focuses on the all-round health condition of structure using structural deformations such as deflections and inclinations or low frequency dynamic responses such as modal properties. This approach is mainly applied to explore the state of whole structure but poses a challenge to localize occurred abnormalities. On the other hand, local SHM mainly assesses regional damages near sensors with high frequency features like electromechanical impedance, elastic waves, and acoustics. It allows easier access to investigate damages occurred on structural members including failure critical members (Park *et al.* 2003, Min *et al*. 2010, Min *et al*. 2012).

KIOST is carrying out extensive studies of the health monitoring of the supporting system of Uldolmok TCPP and making an effort to construct its safety decision algorithm and monitoring system. For this, KIOST fabricated a 1/20 scaled model and various types of SHM approaches and signal processing algorithms were applied on this model. This study proposes a new diagnosis algorithm using the electromechanical impedance as part of this research and this algorithm is also validated on this model. Environmental effects induced by temperature and external loading are real-time compensated with a simple signal processing technique.

## 2. Theoretical backgrounds

### *2.1 Impedance-based SHM*

The electromechanical impedance method utilizes high-frequency structural excitations of surface-bonded piezoelectric patches monitoring changes in structural mechanical impedance. The term of 'electromechanical impedance' stems from two primary properties, i.e., electrical and mechanical impedance. A piezoelectric patch provides a means of coupling the electrical and mechanical impedance, which form a collocated sensor and actuator. There are several types of piezoelectric patches and, among them, MFC (macro fiber composite) patches and PZT (lead(Pb)-zirconate-titanate) ceramic patches are mainly used in the fields of civil, mechanical, and aerospace. Liang *et al*. (1996) performed a one-dimensional coupled electromechanical impedance analysis of an adaptive system driven by a surface-attached piezoelectric patch. Their research first conceptualized that the electromechanical admittance at the terminal of piezoelectric patch reflects the coupled-system dynamics, that is, the electrical admittance $Y(\omega)$, as measured at the terminals of a piezoelectric patch, is directly correlated to the local mechanical impedance of the host structure, $Z_s(\omega)$, and that of a patch, $Z_a(\omega)$.

$$Y(\omega) = G(\omega) + jB(\omega) = j\omega C\left(1 - \kappa_{31}^2 \frac{Z_s(\omega)}{Z_s(\omega) + Z_a(\omega)}\right) \tag{1}$$

where $G$ is the conductance (real part); $B$ is the susceptance (imaginary part); $C$ is the zero-load capacitance of a patch; and $\kappa_{31}$ is the electromechanical coupling coefficient of a patch. Given that the mechanical impedance and the material properties of the patch stay constant, the equation shows that a change in the structure's mechanical impedance directly results in a change in the electrical impedance measured by the patch. Since damages cause a change in the structure's local mass, stiffness, or damping properties and consequently its mechanical impedance, the structure's mechanical integrity can be assessed by monitoring the patch's electrical impedance. It should be noted that the admittance function, $Y(\omega)$, is a complex number. Bhalla *et al.* (2002) demonstrated that the conductance is more sensitively changed due to the structural damage condition as compared to the susceptance. On the other hand, Park *et al.* (2006) found out that the susceptance can be more effectively used for piezoelectric sensor self-diagnosis.

### *2.2 Statistical damage indices for damage detection*

By observing some changes of the electromechanical impedance acquired from a piezoelectric patch attached on a host structure, assessments can be made about the integrity of the host structure. Since the impedance changes provide only a qualitative assessment for damage detection, several scalar damage metrics have been used for quantitative measure of structural damages. Peairs *et al.* (2006) compares several damage metrics, while the most commonly used indices for the impedance method are the root mean square deviation (RMSD) and the cross-correlation coefficient (CC) as

$$RMSD = \sqrt{\frac{\sum_{i=1}^{n}\left\{\mathrm{Re}(Z_0(\omega_i) - \bar{Z}_0) - \mathrm{Re}(Z_1(\omega_i) - \bar{Z}_1)\right\}^2}{\sum_{i=1}^{n}\mathrm{Re}(Z_0(\omega_i) - \bar{Z}_0)^2}} \tag{2}$$

$$CC = \frac{1}{n}\sum_{i=1}^{n}\frac{\left\{\mathrm{Re}(Z_0(\omega_i) - \bar{Z}_0)\right\}\left\{\mathrm{Re}(Z_1(\omega_i) - \bar{Z}_1)\right\}}{\sigma_{Z_o}\sigma_{Z_1}} \tag{3}$$

where $Z_0(\omega)$ is the impedance of the PZT measured in the healthy condition (baseline); $Z_1(\omega)$ is the impedance in the concurrent condition; $n$ is the number of frequency points; $\bar{Z}_0$ and $\bar{Z}_1$ are the mean values of the real parts of $Z_0(\omega)$ and $Z_1(\omega)$ ;and $\sigma_{Z_0}$ and $\sigma_{Z_1}$ are the standard deviations of the real parts of $Z_0(\omega)$ and $Z_1(\omega)$. These metrics are scaled by the baseline measurement, $Z_0(\omega)$, and are corrected for the vertical shift between measurements by subtracting mean values. Upper equations yield a scalar number, which presents the relationship between compared signals. Thus, it is expected that the frequency shift, the peaks splitting, and the appearance of new peaks that appear in the signal will alter the damage metric values and thus alarm the presence of damage (Giurgiutiu 2008). Greater numerical value of the RMSD metric indicates larger difference between the baseline reading and the subsequent reading, which indicates clearer presence of damage in the structure. On the other hand, smaller value of the CC metric indicates larger difference between the impedances and clearer presence of damage.

### *2.3 Effects of temperature and external loading*

Temperature variations due to surrounding changes should be considered with careful attention because the temperature variation causes a marked severe change in the structural dynamic response and also piezoelectric materials exhibit the strong temperature dependency, which may lead to erroneous diagnostic results of real structures(Park *et al*., 1999). To date, several studies have been reported to avoid the temperature variation effects on the impedance measurement. Krishnamurthy *et al*. (1996) demonstrated the effect of temperature on a free piezoceramic patch and found that an increase in the temperature leads to a decrease in the impedance amplitude. Park *et al*. (1999) proposed a compensation technique to minimize the effect of temperature on the impedance of piezoelectric sensor attached on the structure in the range of 26-70°C. Bhalla *et al*. (2002) investigated the influence of the structure-actuator interactions and temperature variation on the impedance signatures. A concept of active component of admittance signatures was introduced to utilize the direct interactive component after filtering the inert component. The active signatures were extracted from the real (resistance) and imaginary (reactance) parts of impedances to reduce the influence of temperature fluctuations on impedances. Koo *et al*. (2009) proposed the effective frequency shift (EFS; $\tilde{\omega}$ ) method in order to compensate temperature effects on impedances, which is based on the frequency shift giving the maximum cross-correlation coefficient between the baseline impedance data, $Z_0(\omega)$, and the concurrent impedance data, $Z_1(\omega)$, as

$$\max CC = \max_{\tilde{\omega}} \left\{ \frac{1}{n} \sum_{i=1}^{n} \frac{\{\mathrm{Re}(Z_0(\omega_i) - \bar{Z}_0)\}\{\mathrm{Re}(Z_1(\omega_i) - \bar{Z}_1)\}}{\sigma_{Z_o} \sigma_{Z_1}} \right\} \tag{4}$$

This proposed index was validated through experimental studies under temperature variations in the range of 16.1 to 28.5°C. Kim *et al*. (2010) proposed a data normalization technique using the kernel principal component analysis (KPCA), which is known as unsupervised least-square support vector machine. Experimental studies on a full-scale aircraft wing section showed that the proposed approach was well-operated under temperature and static loading variations.

Structural components such as slabs, beams, and columns are practically subjected to some form of external loading. It is known that the electromechanical impedance signature obtained on a loaded structure is different from the one without the load. Thus, the influence of external loading on the electromechanical impedance has been examined by several researchers. Abe *et al*. (2000) first proposed a technique to identify in situ stresses in thin structural members through experimental studies. Ong *et al*. (2000) investigated the effects of stresses on the frequency response functions of structures through the 1-D and 2-D simulations. The simulated results showed that when a structure is axially loaded, lateral shifts toward right took place in local natural frequencies of structure (i.e., increases of resonance frequencies) and these shifts were reflected in the electromechanical admittance spectrum. Annamdas *et al*. (2007) presented the influence of loading on electromechanical admittance signatures by experimental and statistical investigations. When a bending moment was applied to both a structure and a PZT by an external static line load, conductance and susceptance signatures shifted upwards from baseline signature. The amount of upward shift seemed to increase with both the increase in magnitude of load and the increase in frequency range. And lateral movements on conductance and susceptance signatures were also observed, which could be explained by a relationship with the structural stiffness of the specimen. They explained this phenomenon occurred because the applied external load acted as interference in the wave propagation. The change of signature due to the external load was observed in the susceptance much clearly than in conductance, and they concluded that the susceptance signature is a better indicator than the conductance signature for detecting stress in the structure. They also investigated the effect of boundary condition. Various boundary conditions were applied to the beam-type specimen. Results showed that there was not much difference between the signature for the simply supported condition and that for the free-end condition. However, the signature for the fixed-fixed condition showed differences from those two signatures. They supposed it occurred because stresses were built in the specimen due to end restrains. Lim *et al*. (2011) proposed a new data normalization technique using KPCA to improve damage detect ability under varying temperature and external loading conditions and to minimize false alarms due to these variations. Experimental studies were carried out on a lab-scale metal fitting lug and applied to a full-scale composite wing specimen with a complex geometry. Results of the proposed method were compared with those of conventional methods and showed that it could correctly detect damages under various environmental conditions including temperature variations and static/dynamic loadings.

## 3. Conventional SHM for lab-scale tidal current power plant structure

### *3.1 Experimental setup*

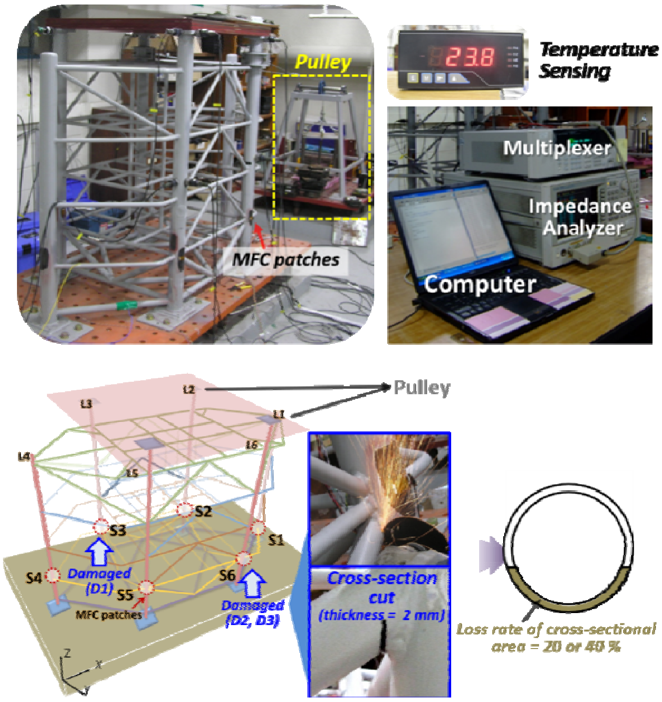


Fig. 1 1/20-scaled model of Uldolmok TCPP and measurement system thereof

One of critical issues on TCPP is to monitor and secure structural safety because TCPP is generally constructed under severe environmental conditions such as high speed of current and excessive current loading so that it is difficult to control the construction process accurately. In this study, an impedance-based SHM is performed on a 1/20-scaled model of the Uldolmok TCPP and aims to alarm the structural local failure on welded joints under changes in temperature and transverse loading which simulates real environmental loading cases.

Fig. 1 shows a target structure for this study which is an1/20-scaled model. The reduction ratio was decided as 1/20 in length just considering the structural size because the law of similarity may not be generally required in SHM studies. With this, the reduction ratio in dead load corresponds to 1/8,000 and the stiffness should be reduced to 1/400 provided the same material is used in the scaled model. However, since structural steel used in Uldolmok TCPP could not be supplied in small quantity, the scaled model was manufactured with commercial steel pipes made of general carbon steel (KSD3566) with the consideration of the reduction ratio in stiffness. Steel plates were located on the main supporting frame with the reduction ratio in weight of 1/8,000 for simulating structures located on the TCPP such as generating units and houses which contributes to the mass increase without effects on structural stiffness or bearing-capacity.

This model was mainly supported with six jacket legs (L1~L6), the diameter of which was 76.3 mm and fixed to the steel support slab with bolts. To measure electromechanical impedances for local SHM, six MFC patches (Smart Materials Inc., Model. 2814P1 in which 28 and 14 means the length and width in mm) were attached on each leg at a height of 340 mm above the support slab corresponding to DL-14 m in reality (S1~S6). An MFC patch is quite flexible so that it can be easily attached on a curved surface but has quite lower performance compared to a PZT patch. These patches were connected to a conventional impedance measuring device (Agilent 4294A) through a multiplexer (Agilent 34980A) and impedance signatures from them were measured and stored in computer in order of precedence with displaying graph of raw signals. On the other hand, indoor temperature data were also measured with temperature measuring unit (Keiki A5113-13).

Temperature and static transverse loading were considered as environmental factors in this study. Indoor temperature was controlled with both an air-conditioner and an electric heater located at approximately 1.5 m far from the target structure within the rage of 20.4 to 30.1°C as in Fig. 2(a) considering that the annual average difference between the highs and the lows in water temperature of Uldolmok was around 10°C. And transverse loading of tides in real offshore structures was simulated by using a steel pulley tied at the top of two jacket legs, L2 and L6, controlling the eccentric force carefully. The KIOST performed on-the-spot survey in 1992 and 2002 for design and construction of Uldolmok TCPP and it showed that the mean flow velocity was 2.38 m/s at 5 m from ground and 2.73 m/s at 25 m from ground showing a bit of a difference depending on the depth of water. The maximum current speed was observed as 6.3 m/s at the center of narrow channel under Jindo Bridge. Based on the observation data near the Uldolmok TCPP, the design flow velocity was decided as 5.3 m/s, which corresponds to the design current loading of 10,375 kN and about a third of the total weight of structure (Yi *et al*. 2009). In this study, transverse loading of 3.06 kN, a third of the total weight of the scaled-model, was applied to the structure and Fig. 2(b) shows an example of one cycle loading.

Damages on offshore structures such as joint cuttings, fatigue cracks, and corrosions are caused by material deterioration, mistakes on welding and fabrication process, excessive vibration due to pile driving, dragging of structural members on the move or during installation, collision with ships or floating matters, or reduced corrosion prevention system (Wintle *et al*. 2005, Puskar *et al*. 2006, Spong *et al*. 2006). In this study, crack damages was simulated at welded joints connecting leg and bracing members.

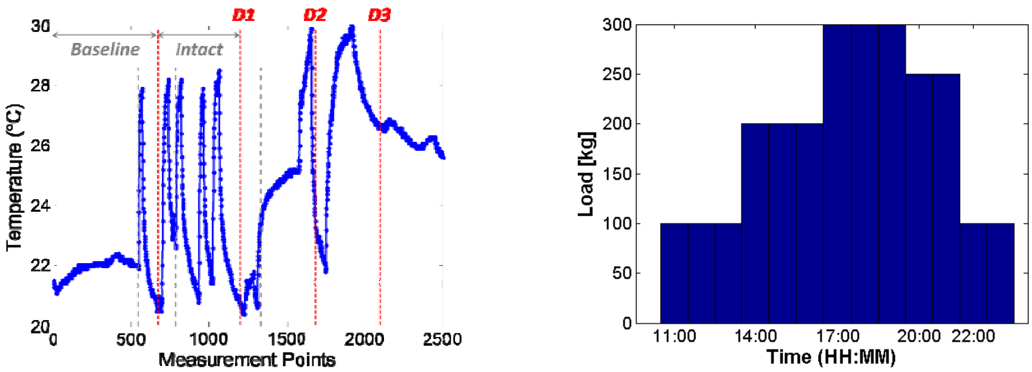


(a) Temperature changes during tests

(b) One cycle transverse loading

Fig. 2 Environmental changes on the target structure

Table 1 Experimental damage scenarios

| Index | Period (days) | Temperature change (°C) | Loading (cycle) | Damage type | Measurement point |
|---|---|---|---|---|---|
| Baseline 1 | 5.4 | 0.8 | 2 | None | 518 |
| Baseline 2 | 1.5 | 7.4 | 1 | None | 144 |
| Intact 1 | 1.0 | 7.7 | 0 | None | 96 |
| Intact 2 | 4.5 | 8.0 | 3 | None | 432 |
| Damage 1-1 | 1.1 | 1.4 | 0 | D1(near L3) | 105 |
| Damage 1-2 | 4.1 | 9.3 | 1 | D1(near L3) | 393 |
| Damage 2 | 4.3 | 8.3 | 1 | D2(near L6) | 412 |
| Damage 3 | 4.2 | 1.3 | 1 | D3(near L6) | 400 |

The long-term performance of MFC patches attached on the structure was investigated in detecting crack and cutting damage at structural members or welded joints under various environmental conditions. Artificial damage (D1~D3) was induced at a height of 340 mm above the support slab as shown in Table 1. Here, D1 is 20 % cross-section cut at welded joints between L3 and diagonal bracing member which is 10 cm from S3, D2 is 20% cross-section cut at welded joints between L6 and diagonal bracing member which is 5 cm from S6, andD3 is 40% cross-section cut at the same location with D2.Note that the damage severity was calculated by the loss rate of cross-sectional area. Damage was induced. Experiments were performed in various scenarios with changes in temperature and loading conditions and different damage cases and it was summarized in Table 1.

### *3.2 Measured impedance signatures*

Impedance signals were measured through 6 MFC patches in frequency ranges of 28.5~48.5 kHz every 15 minutes and monitored during around 26 days. The frequency range was chosen as it includes several resonant peaks related to the dynamic interaction between the piezoelectric patch and the structure (Park *et al*. 2003). Once about 662 impedance signatures were obtained during 6.9 days for baseline when no damage was induced in order to investigate only environmental effects. Baseline 1 is case of only loading under constant temperature, and Baseline 2 is case of changes in both loading and temperature. After baselines were build up, actual tests started and impedance signals were measured according to the scenarios in Table 1 as inducing damages under temperature and loading control. Fig. 3(a) shows resistance signals measured through S1 in baseline, which changed largely purely due to environmental conditions, especially temperature variations. From this figure, it was found that the signal shifts rightwards with a small variation in magnitude as the temperature increases. It should be noted that vertical shifts of signatures may be caused by a change in environmental conditions or a piezoelectric patch itself which can be easily corrected by subtracting mean values from the interrogation impedance (Park *et al*. 2003).

When 20% and 40% section cut at welded joints between L6 and diagonal bracing member (D2 and D3), the resistance signal from S6 was displayed in Fig. 3(b). The induced damage in the same temperature condition of 25.4°C mainly affected on the signal magnitude depending on the damage severity while the change in temperature of 5.4 °C was closely related to the signal shift along the frequency axis. Distinctive changes in signals were not observed in these series of experiments, which was supposed that the size of MFC patch is too small compared to that of target structure because the smaller commercial patch in general has lower material constants related to impedances. This problem would happen on SHM of full-scale structure equipped with piezoelectric patches, but it is expected to be solved by improving patch capacity and increasing size for sufficient actuation performance.

### *3.3 Conventional approach for long-term SHM*

A conventional CC and max CC indices in Eqs. (2) and (3) have the value of between 0 in completely damaged case and 1 in intact case, but in this study they were replaced into 1-CC and 1-maxCC for convenience. So these modified indices have the value of 0 in case of intact condition and increase gradually with the severe signal change.

Figs. 4(a) and 4(b) displayed 1-CC and 1-maxCC indices with varying temperature. Here, bold dot lines indicate points where a damage was induced (D1~D3). When only loading was applied without temperature and structural changes, 1-CC and 1-maxCC indices remained constant with small fluctuation (Baseline 1).However, they significantly responded to temperature variation seven though the max CC was used for compensating the temperature effect. On the other hand, it seemed to have a trend that 1-CC values follow temperature variations. Both 1-CC and temperature were displayed together in Fig. 4(c) to check the trend, but they did not show clear relationship.

From these results, it could be found that (1) the external loading is not a severer factor than temperature when both changes in loading and temperature are applied together and (2) the max CC index has a limitation under varying temperature conditions and even causes positive or negative false alarms. Therefore other approaches are needed for the reliable impedance-based long-term SHM to secure correct diagnosis results.

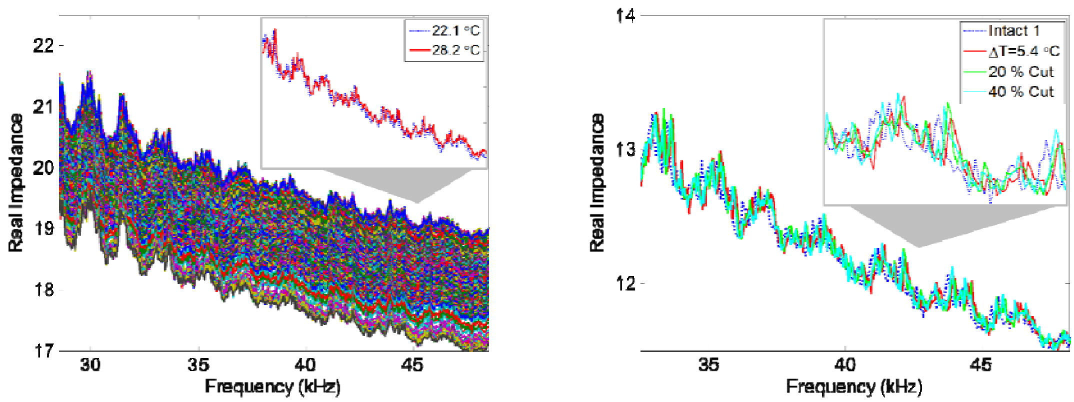


(a) Baselines (b) Damaged cases

Fig. 3 Examples of measured impedance signals

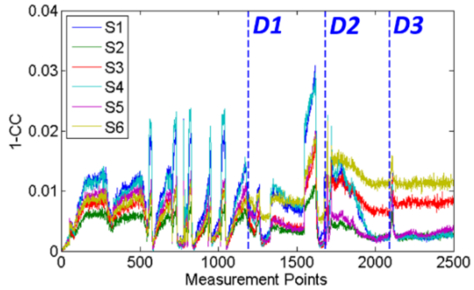


(a) Changes in CC values

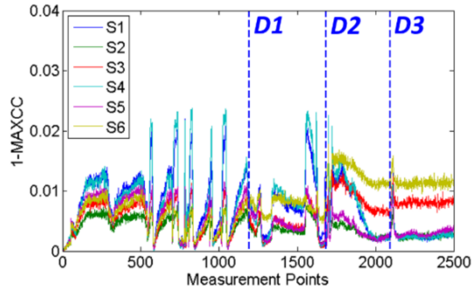


(b) Changes in max CC values

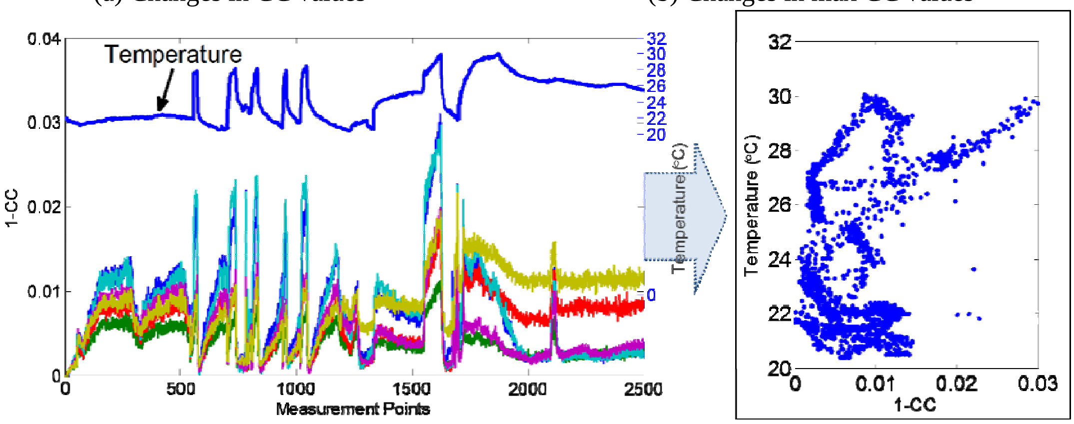


(c) Relation between CC index and temperature

Fig. 4 CC values with various experimental scenarios

## 4. Proposed SHM approach for compensating temperature and loading effects

### *4.1 Principal component analysis*

A principal component analysis (PCA) is a classical method of multivariate statistical analysis that linearly transforms an original set of variables into a substantially smaller set of uncorrelated variables that may represent most of the information in the original set of variables (Jlooiffe 1986 Dunteman 1989), based on the fact that a small set of uncorrelated variables is much easier to understand and use in further analysis than a larger set of correlated variables. Unwanted noises could be reduced through data compression. Thus this technique has been widely applied to virtually every substantive area including engineering, biology, medicine, chemistry, meteorology, geology, behavioral and social sciences, etc.

The original set of variables ($x_1, x_2, \cdots, x_N$)in an $N$-dimensional space is transformed into a new set of uncorrelated variables ($z_1, z_2, \cdots, z_P$), the so-called principal components (PCs), in a $P$-dimensional space ($N > P$) with an orthogonal projection. When $M$ sets of data were measured, $\{x\}_j$ ($j = 1, 2, \cdots, M$), a covariance matrix $[C]$ can be constructed as

$$[C] = \frac{1}{M-1}\sum_{i=1}^{M}\left(\{x\}_j - \{\bar{x}\}\right)\left(\{x\}_j - \{\bar{x}\}\right)^T \tag{5}$$

where $\{\bar{x}\}$ is the mean of $\{x\}$. Then a singular value decomposition of $[C]$ is

$$[C] = [A][\Lambda][A]^T \tag{6}$$

where $[A]$ is the eigen-matrix, and $[\Lambda]$ is the diagonal matrix with the eigen-values. The transformation to the principal component $\{z\}$ is then accomplished as

$$\{z\}_j = [A]^T\left(\{x\}_j - \{\bar{x}\}\right) \tag{7}$$

This study applied this PCA to eliminate environmental effects on damage indices calculated from impedance signals, especially temperature, as well as unwanted noises and to reduce the data dimensionality which can be used usefully in wired/wireless data communication. A damage index matrix, $[DI] = DI_{ij}\ (i = 1,2,\cdots,N;\ j = 1,2,\cdots,6)$, which consists of $N$ damage index values from 6 MFC patches, can be expressed the linear combination of the principal component vectors (eigen-vectors), $\{z\}_j = \{z_{j1}, z_{j2}, \cdots, z_{j6}\}^T\ (j = 1,2,\cdots,6)$, and their coefficient vectors, $\{a\}_j = \{a_{j1}, a_{j2}, \cdots, a_{jN}\}^T\ (j = 1,2,\cdots,6)$ as

$$[DI] = \sum_{i=1}^{M} a_j z_j^T \tag{8}$$

Since the principal component vectors are orthogonal each other, the $\{a\}_j$ can be obtained as

$$\{a\}_j = [DI]z_j \tag{9}$$

If unknown unwanted components such as environmental effects are mainly included in the $i$ -th PC, those can be eliminated from $[DI]$by using the $i$-th principal component vector and its coefficient vector. Then, a$[DI]'$ index is drawn as a new damage index as in Eq. (10). It is noted that great care is required in order to determine the number of PCs which has to be eliminated from data.

$$[DI]' = [DI] - [DI]z_i z_i^T \tag{10}$$

Both 1-CC and 1-maxCC indices were used for $[DI]$in this study and critical PCs governed by temperature and external loading effects were investigate and then eliminated from original data to long-term monitor the target structure with reliable evaluation.

### *4.2 Proposed SHM approach for long-term SHM*

The PCA was first performed using baseline signals (Baseline 1 and 2) obtained from six MFC patches and then six PC vectors, $\{z\}_j\ (j = 1,2,\cdots,6)$, were extracted. Since temperature and external loading effects were included in each PC with different contributions, it might be very critical to obtain lots of baseline data as well as to select PCs for damage diagnosis. Here, it should be noted that around 662 baseline data were obtained for 6.9days. After investigating the relationship between each PC and environmental effects, especially temperature variations, it was found that the first PC and the second PC were mainly governed by the temperature variation trend as shown in Figs. 5(a) and 5(c). Once the first PC was removed from the original 1-CC index, calibrated results were displayed in Fig. 5(b). As shown in this figure, large fluctuations due to temperature changes in baseline reduced and the damage index values increased enough to recognize the subsequent damages indicating that unknown damages occurred near S3 and S6. However the fluctuations still remained considerable and caused frequent false positive alarms. Changes in index values of S3 due to a cut damage near S3 were even smaller than those due to temperature changes. The values of S1, S2, S4, and S5, varied in cases of D1-D3 although these patches were placed at different structural members far from damage locations. It was supposed that the internal stress was redistributed by the damages. Moreover, since each patch responded to a near-structural change with different sensitivity, it seemed to be hard to evaluate the damage severity and location quantitatively by direct comparison of the index value each other when multiple patches were used for SHM. In-depth studies on this sensor calibration should be performed further considering the bonding condition to provide much useful information.

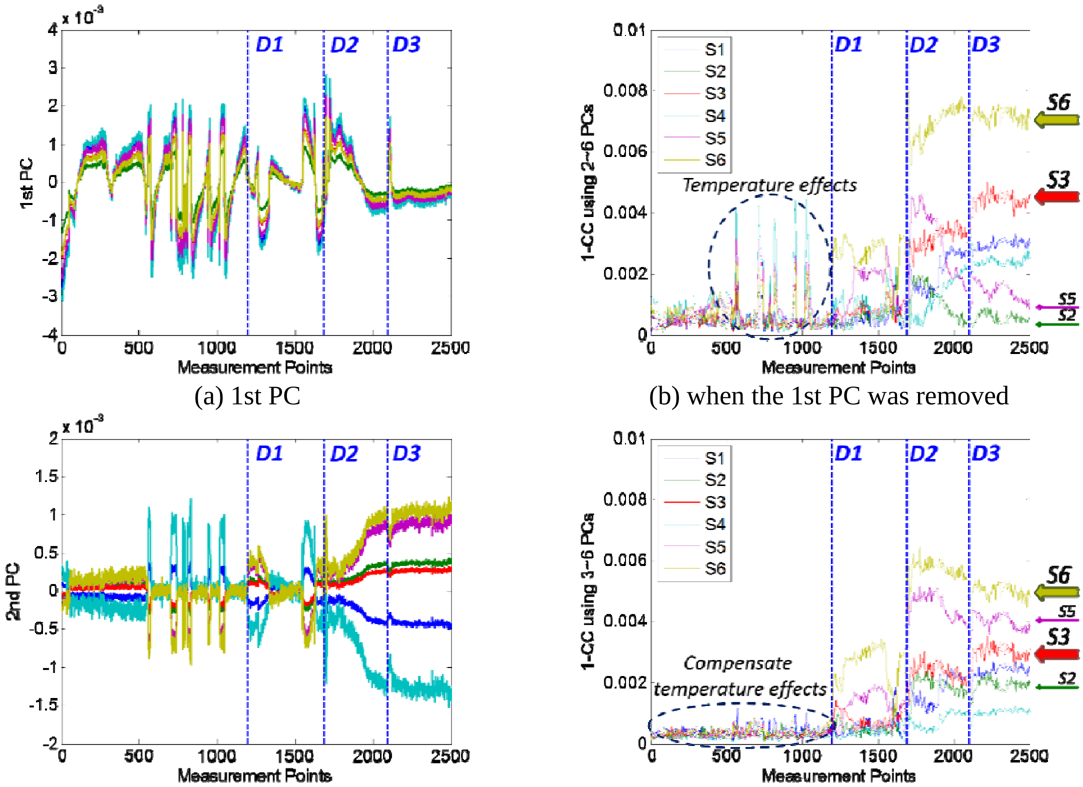


(a) 1st PC (b) when the 1st PC was removed

(c) 2nd PC (d) when the 1st and 2nd PCs were removed

Fig. 5 Modified damage indices employing the principal component analysis

The first and second PCs were then eliminated from original 1-CC data and the results were shown in Fig. 5(d). The initial fluctuation in baseline induced by the temperature decreased distinctively compared to Fig. 5(b) indicating the temperature mainly affected the second PC more than the first PC. Thus, after removing the second PC, the damage case of D1 occurred near S3 was clearly detected with an abrupt increase of damage index above the threshold level in baseline, although overall changes in stress distribution and structural status were observed, not limited to the index of S3. Moreover it was founded by trials with the combination of PCs that PCs except the first two PCs were not sensitive to environmental changes and did not largely affect the diagnosis results in the case of when the first two PCs were utilized. From these results, it was decided that the use of the first two PCs was the optimum solution to reduce environmental effects in the impedance signals.

To investigate in-detail variations of index values of all patches, they were displayed in Fig. 6 with the location of the MFC patch. In the case of D1, S1 and S4 did not show noticeable turning point by the induced damage while index values of other patches varied. S5 and S6 had much larger values than S3 nearest patch from the induced damage, which was thought to be due to the patch sensitivity as mentioned above, and these were even more sensitive to structural changes than environmental changes. When a cut damage occurred near S6 (D2), all patches responded and gave an alarm that an unknown change happened supposing that it would be near S6. However a severer damage near S6 (D3) did not make index values of S5 and S6 increased. Considering the impedance signal is related to the local dynamic mode of structure, it can happen because the damage index may remain unaffected by the damage severity when the damage location is identical.

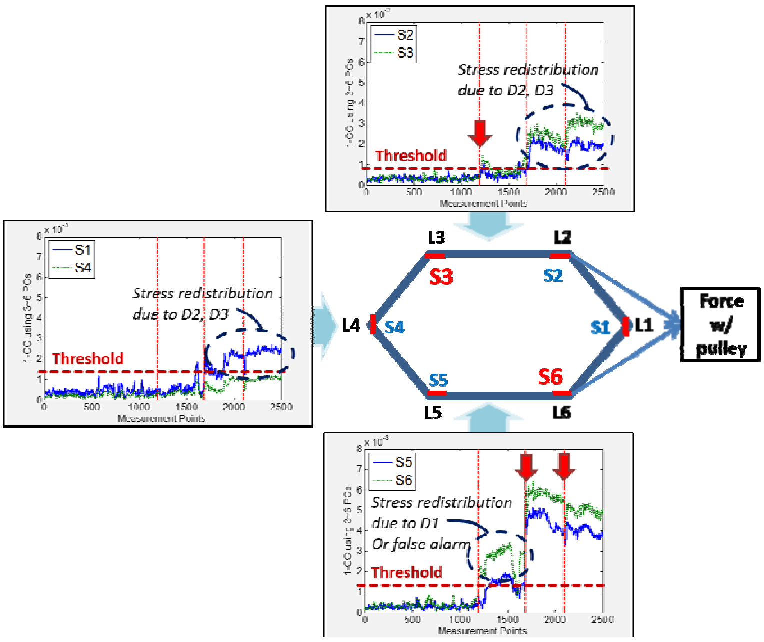


Fig. 6 Modified CC damage index after removing the first and second principal components

## 5. Conclusions

This study proposed a PCA-based method to compensate unknown environmental effects, especially temperature effects, and to provide only damage-sensitive features in the long-term SHM using impedance signals. A 1/20-scaled model of an Uldolmok current power plant structure in South Korea was made and monitored during around 26 days inducing several cut damages under varying temperature and transverse loadings. Impedance signals were measured periodically and conventional damage indices such as CC and max CC were calculated. However they showed large fluctuations in spite of no damage cases and provided lots of false alarms especially with temperature changes. To tackle this problem, components sensitive to these environmental changes were first separated from the damage index values through PCA and then eliminated. In this study, they were the first and second PCs. The final calibrated results showed that the environmental effects diminished clearly showing a potential of the proposed approach as a tool for long-term SHM under significant environmental changes, although there are problems to be ironed out further including the sensor calibration with different bonding condition for damage quantification.

## Acknowledgements

This research was a part of the project titled “Development of active-controlled tidal stream generation technology” funded by the Ministry of Oceans and Fisheries, Korea (20110171) and KIOST research program (PE99322). The authors would like to express their appreciation for the financial support.

## References

Abe, M., Park, G. and Inman, D.J. (2000), “Impedance-based monitoring of stress in thin structural members”, *Proceedings of the 11th International Conference on Adaptive Structures and Technologies*, Nagoya, Japan.

Annamdas, V.G.M., Yang, Y. and Soh, C.K. (2007), “Influence of loading on the electromechanical admittance of piezoceramic transducers”, *Smart Mater. Struct.*, **16**(5), 1888-1897.

Bhalla, S., Naidu, A.S.K. and Soh, C.K. (2002), “Influence of structure-actuator interactions and temperature on piezoelectric mechatronic signatures for NDE”, *Proceedings of the ISSS-SPIE Int'l Conferences on Smart Materials Structures and Systems*, Bangalore, India.

Dunteman, G.H. (1989), *Principal Components Analysis*, Sage Publications, London.

Giurgiutiu, V. (2008), *Structural Health Monitoring With Piezoelectric Wafer Active Sensors*, Academic Press, USA.

Jlooiffe, I.T. (1986), *Principal Component Analysis*, Springer, New York.

Kim, M.K., Lim, H.J., Sohn, H. and Park, C.Y. (2010), “Impedance-based bolt loosening detection under varying temperature and loading”, *Proceedings of the Asian Pacific Workshop on Structural Health Monitoring*, Tokyo, Japan.

Koo, K.Y., Park, S., Lee, J.J. and Yun, C.B. (2009), “Automated impedance-based structural health monitoring incorporating effective frequency shift for compensating temperature effects”, *J. Intel. Mat. Syst. Str.*, **20**, 367-377.

Krishnamurthy, K., Lalande, F. and Rogers, C.A. (1996), “Effects of temperature on the electrical impedance of piezoelectric sensors”, *Proceedings of the SPIE Smart Structures and Materials: Smart Structures and*

*Integrated Systems*, **2717**, 302-310.
Liang, C., Sun, F.P. and Rogers, C.A. (1996), "Electro-mechanical impedance modeling of active material systems", *Smart Mater. Struct.*, **5**(2), 171-186.
Lim, H.J., Kim, M.K., Sohn, H. and Park, C.Y. (2011), "Impedance based damage detection under varying temperature and loading conditions", *NDT & E Int.*, **44**(8), 740-750.
Min, J., Yun, C.B., Park, S., Lee, C.G. and Lee, C. (2012), "Impedance-based structural health monitoring incorporating neural network technique for identification of damage type and severity", *Eng. Struct.*, **39**, 210-220.
Min, J., Park, S., Yun, C.B. and Song, B. (2010), "Development of a low-cost multifunctional wireless impedance sensor node", *Smart Struct. Syst.*, **6**(5-6), 689-709.
Ong, C.W., Yang, Y.W., Naidu, A.S.K., Lu, Y. and Soh, C.K. (2002), "Application of the electro-mechanical impedance method for the identification of in situ stress in structures", *Proceedings of the SPIE Conference on Smart Structures, Devices, and Systems.* 4935, San Diego, CA.
Park, G., Kabeya, K., Cudney, H.H. and Inman, D.J. (1999), "Impedance-based structural health monitoring for temperature varying applications", *JSME Int. J. Series A*, **42**(2), 249-258.
Park, G., Sohn, H., Farrar, C.R. and Inman, D.J. (2003), "Overview of piezoelectric impedance-based health monitoring and path forward", *Shock Vib. Digest*, **35**(6), 451-463.
Park, G., Farrar, C.R., Rutherford, A.C. and Robertson, A.N. (2006), "Piezoelectric active sensor self-diagnostics using electrical admittance measurements", *J. Vib. Acoust.*, **128**(4), 469-476.
Peairs, D.M., Tarazaga, P.A. and Inman, D.J. (2006), "A study of the correlation between PZT and MFC resonance peaks and damage detection frequency intervals using the impedance method", *Proceedings of the International Conference on Noise and Vibration Engineering*, Leuven, Belgium.
Puskar, F.J., Spong, R.E. and Ku, A. (2006), "Assessment of fixed offshore platform performance in hurricane ivan", *Proceedings of the Offshore Technology Conference*, Houston, Texas, USA.
Spong, R.E. and Puskar, F. (2006), *Assessment of fixed offshore platform performance in hurricanes andrew, Liliand Ivan*, Report. MMS Project No. 549, Energy Engineering Inc., Houston,Texas.
Wintle, J.B. and Pargeter, R.J. (2005), "Technical failure investigation of welded structures (or how to get the most out of failures)", *Eng. Fail. Anal.*, **12**(6), 1027-1037.
Yi, J.H., Park, W.S., Park, J.S. and Lee, K.S. (2009), "Structural health monitoring system for 'Uldolmok' tidal current power pilot plant and its applications", *Proceedings of the ASME International Conference on Ocean, Offshore and Arctic Engineering*, Hawaii, USA.